



Simulating potential response of hydrology, soil erosion, and crop productivity to climate change in Changwu tableland region on the Loess Plateau of China

X.-C. Zhang^{a,*}, W.-Z. Liu^{b,c}

^a USDA-ARS Grazinglands Research Laboratory, 7207 West Cheyenne St., El Reno, Oklahoma 73036, USA

^b Institute of Soil and Water Conservation, Chinese Academy of Sciences and Ministry of Water Resources, Yangling, Shaanxi 712100, PR China

^c College of Resources & Environmental Science, Northwest Sci-Tech University of Agriculture and Forestry, Yangling, Shaanxi 712100, PR China

Received 11 January 2005; accepted 18 May 2005

Abstract

Knowledge of the impacts of climate change on agro-ecosystems is needed for developing optimal conservation and production practices. The objective of this study was to evaluate the potential impacts of projected climate changes during 2070–2099 under three emissions scenarios (A2a, and B2a, and GGA1) on hydrology, soil loss, and crop production in Changwu tableland region on southern Loess Plateau of China. Monthly projections for the periods of 1950–1999 and 2070–2099 were used from the Hadley Centre's general circulation model (HadCM3). A stochastic weather generator (CLIGEN) was used to downscale monthly HadCM3 projections to daily values at three spatial scales. The Water Erosion Prediction Project (WEPP) model was run for a wheat–wheat–maize rotation under conventional and conservation tillage at the 8.7% and 17.6% slopes. HadCM3 predicted a 23–37% increase in annual precipitation, 2.3–4.3 °C rise in maximum temperature, and 3.6–5.3 °C rise in minimum temperature for the region over the century. Compared with the present climate, predicted percent increases under climate changes, as averaged over the three spatial scales for each emissions scenario and slope, ranged from 29 to 79% for runoff, 2 to 81% for soil loss, 15 to 44% for wheat grain yield, 40 to 58% for maize yield, 25 to 28% for crop transpiration, 21 to 34% for soil evaporation, and 4 to 12% for long-term soil water reserve under the conventional tillage. However, adoption of the conservation (delayed) tillage could reduce runoff by 18–38%, and decrease soil loss by 56–68% as compared to the conventional tillage under the present climate. These results suggest that the use of the conservation tillage would be sufficient to maintain low runoff and erosion levels and thus protect agro-ecosystems under projected climate changes.

© 2005 Elsevier B.V. All rights reserved.

Keywords: Climate change; Soil erosion; Soil water balance; Surface hydrology

* Corresponding author. Tel.: +1 405 262 5291; fax: +1 405 262 0133.

E-mail address: jzhang@grl.ars.usda.gov (X.-C. Zhang).

1. Introduction

The review of “Climate Change 2001: The Scientific Basis” prepared by the Intergovernmental Panel on Climate Change (IPCC Working Group I, 2001) has concluded that globally averaged mean evaporation, precipitation amount, and rainfall intensity will very likely increase in response to increased concentrations of greenhouse gases in the atmosphere. The upward trend in total precipitation and a bias toward more intense rainfall events are of great concerns when assessing the potential impacts on soil erosion, water resources, and ecosystems, because most soil loss and environmental damage are caused by infrequent severe storms (Edwards and Owens, 1991; Zhang and Garbrecht, 2002). The potential for such projected climate changes to increase the risk of soil erosion and related environmental consequences is clear, but the potential damages in particular regions need to be assessed (SWCS, 2003). This information is helpful in determining (i) whether a change in soil and water conservation practices is warranted under climate change and (ii) what practices should be taken to adequately protect soil and water resources if a change is warranted.

Climate change can affect soil erosion and hydroecology through multiple pathways because the effects of many climatic variables such as precipitation, temperature, and CO₂ concentration as well as their interactions are often complex, dynamic, and nonlinear. A change in precipitation, for example, affects soil erosion, runoff, and crop growth differently for a change in frequency versus in severity. A change in temperature affects crop growth differently for a change in minimum versus maximum temperature. The actual impacts of individual variables and/or their interactions, which may differ seasonally and geographically, can only be adequately assessed at a complex system level, and agricultural systems models that mimic the entire agro-ecosystems are powerful tools for attacking such complex issues.

The Water Erosion Prediction Project (WEPP) model is a continuous daily simulation model (Flanagan and Nearing, 1995). It contains erosion, hydrology, climate, daily water balance, plant growth, and residue decomposition components. The plant growth and water balance components were modified to account for the CO₂ effects on evapotranspiration

(ET) and biomass production as described by Favis-Mortlock and Savabi (1996). The modified CO₂-sensitive version was used to study the impacts of climate change on runoff and erosion (e.g., Savabi et al., 1993; Pruski and Nearing, 2002a,b; Zhang et al., 2004). Favis-Mortlock et al. (1991) and Boardman and Favis-Mortlock (1993) evaluated the impacts on runoff and soil erosion using the Erosion Productivity Impact Calculator (EPIC). Overall results from all those studies indicated that a 1% increase in precipitation would result in a 0.5–4% increase in soil loss and a 1–4% increase in surface runoff. In addition, the impacts of projected climate change on crop productivity were evaluated in-depth using other agricultural systems models by many researchers (e.g., Rosenzweig and Parry, 1994; Semenov and Porter, 1995; Mearns et al., 1997; Mavromatis and Jones, 1998; Mavromatis and Hansen, 2001a,b).

The major obstacles for impact assessment are the spatial and temporal scale mismatches between coarse resolution projections of general circulation models (GCMs) and fine resolution data requirements of agricultural systems models (Hansen and Indeje, 2004). Both dynamic and empirical (statistical) approaches are used to bridge the spatiotemporal gaps. Dynamic downscaling is used to achieve higher spatial resolutions by nesting regional climate models (RCMs) within GCM output fields. Statistical techniques in principle fall in three categories: weather generators, transfer functions, and weather typing schemes (Wilby et al., 1998). The transfer function approach involves deriving statistical relationships between observed local climatic variables (predictands) and large scale GCM output (predictors) using regression-type methods such as multivariate linear or nonlinear regressions (Solman and Nuñez, 1999; Wilby et al., 1998). Statistical temporal-downscaling or disaggregation is often achieved using stochastic weather generators by perturbing the present climate under the guidance of GCM-projected relative changes (e.g., Wilks, 1992; Katz, 1996; Mavromatis and Jones, 1998; Zhang et al., 2004).

Precise impact assessment at particular locations or in small watersheds requires accurate spatial downscaling of GCM projections. However, considering uncertainty inherent in the choice of GCMs and greenhouse gas forcing scenarios and the fact that the skillful scale (spatial scales of aggregation at which

errors between GCM-projections and observations are acceptable for a particular application) is likely larger than the native scale of GCMs, Hewitson (2003) suggested that impact assessment should first focus on examining the regional sensitivity to larger scale climate perturbations. Hewitson further proposed an approach to first developing larger-scale climate perturbations over multiple GCM grid cells and then applying the aggregated perturbations to observational data at any spatial scale including a weather station. This approach, sidestepping the need for accurate spatial downscaling, tends to provide a more reliable assessment of the first-order sensitivity of regional responses to climate changes. A similar approach was used by Zhang (2005) to assess the impact of climate change on soil erosion and wheat production at varying regional scales.

Zhang et al. (2004) developed a downscaling method that can be used to directly incorporate changes in monthly precipitation and temperature distributions including mean and variance into daily weather series using a stochastic weather generator (CLIGEN) developed by Nicks and Gander (1994). Their test results indicated that the method was satisfactory in transferring interannual monthly variabilities of precipitation and temperature to daily weather series, and that an increase in projected precipitation variance, which increased the occurrence of large storms, substantially increased predicted soil loss and surface runoff in conventional tillage winter wheat in Oklahoma.

Climate change scenarios used in this study were from the recent climate change experiments conducted using a third generation general circulation model (HadCM3) at the Hadley Centre, UK (Wood et al., 1999; Gordon et al., 2000; Pope et al., 2000). The HadCM3 climate change experiments issued monthly projections for the next 100 years for the entire globe. The greenhouse gas emissions scenarios of A2a, B2a, and GGA1 were selected to represent relatively high, low, and intermediate CO₂ increases, respectively. Each scenario described a possible demographic, economic, societal, and technological future. Selection of the HadCM3 model was subjective, and other GCM models and emissions scenarios may also be used. It should be mentioned that future climate projections of different GCMs are similar at the global level, but may differ in particular

regions. Thus, the impacts on hydrology and soil erosion in a particular region would be different when different GCMs are used. Since this is an exploratory study, the projections of the HadCM3 model were only used. In the future study, outputs from other GCMs will be included.

The Loess Plateau, which occupies 380,000 km² (Chen et al., 1988), is situated in the middle reaches of the Yellow River. It is covered with loose, fine, uniform, and highly erodible aeolian deposits. The climate varies from semiarid to subhumid, with heavy storms mostly falling in July through September. It is one of the most eroded regions in the world because of highly erodible soils, steep slopes, heavy storms, and low vegetation cover stemming from intensive cultivation and improper land uses. On average, about 1.53 billion tonnes of suspended sediment were eroded from the Loess Plateau each year (equivalent to 5–6 mm soil depth), and were delivered to the lower reaches of the Yellow River (Chen et al., 1988). About a quarter of the suspended sediment (0.4 billion tonnes) was deposited on the riverbed in the lower reaches, which are 3–12 m above the ground and is rising at 8–10 cm each year (Chen et al., 1988). The prominent problems of flood control in the lower reaches of the Yellow River and soil deterioration resulting from soil erosion in the middle reaches are of great concerns to the Chinese government. In past decades, the Chinese government has launched several national projects aimed at controlling and alleviating the problems through research, education, extension, and implementation of comprehensive control measures, and great progress has been made. However, the potential impacts of climate change on the fragile and vulnerable ecosystems on the Loess Plateau may further complicate and exacerbate the existing problems. Zhang et al. (2005) reported that rainfall erosivity, which is the main erosive force causing soil erosion, would increase between 8 and 35% on the Loess Plateau in the next 100 years based on the HadCM3 A2 and B2 projections. How climate change will impact surface hydrology, soil erosion, and crop production on the Loess Plateau is of great interest to scientists and policymakers for developing sustainable conservation strategies for the region. To date, limited research in this regard has been conducted and reported in the literature.

The objectives of this study were to evaluate the potential regional impacts of HadCM3-projected climate changes during 2070–2099 under A2a, and B2a, and GGA1 forcing on surface hydrology, soil erosion, and crop productivity in Changwu tableland region on the Loess Plateau of China using the CLIGEN and WEPP model, and to test the feasibility and applicability of the CLIGEN for use in climatic impact assessment on the Loess Plateau.

2. Materials and methods

2.1. Site description

The Changwu experiment station is located at 35.2°N and 107.8°E (Fig. 1). The elevation is about 1206.5 m above sea level. The prevailing landform is loessial tableland. The loess is more than 100-m thick on the tableland. The soil is predominantly silt loam with silt content greater than 50% (two soil series: Huangmiantu and Heilutu). The average annual precipitation is 578 mm, with 55% falling in July through September. The annual average temperature is 9.2 °C. The common regional cropping system is a three-year rotation of winter wheat–winter wheat–summer maize. Rainfed agriculture is the dominant production system.

2.2. WEPP calibration

Measured soil, climate, crop management information, surface runoff, and sediment yield from 1988 to 1992 were used to calibrate soil erodibility parameters of the WEPP model (v2004.7), which was modified to incorporate the effect of elevated CO₂ on plant growth and evapotranspiration. Measured properties of the Huangmiantu soil included soil texture, organic matter content, bulk density, hydraulic conductivity, wilting point water content, and field capacity of the soil profile (Table 1). Daily precipitation amount, rainfall duration, rainfall intensity, maximum and minimum temperature were measured. Two field runoff plots and two cropping systems were selected. One runoff plot (20.1 m long by 5 m wide with a 8.7% slope) was under conventionally tilled continuous bare fallow. Another plot (20.3 m long by 5 m wide with a 17.6% slope) was under conventionally tilled continuous soybean with residue removed after harvest. Soybean seed yield was calibrated to the average yield of the region. Soil erodibility was calibrated for the soil on both plots under the condition that measured average annual runoff matched WEPP-predicted runoff. Calibrated critical shear stress was 3.5 Pa, and interrill and rill erodibility were $1.5 \times 10^6 \text{ kg s m}^{-4}$ and 0.0025 s m^{-1} , respectively. The measured and cali-

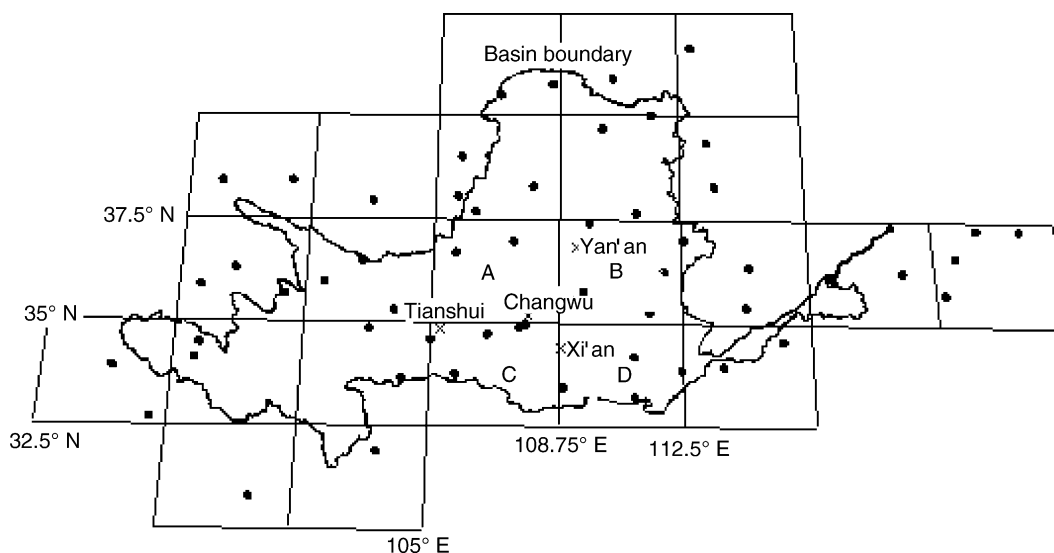


Fig. 1. The Yellow river basin and GCM grid cells, showing the site and four grid cells used in this study. Revised after Fig. 3 of Zhang et al. (2005).

Table 1
Soil properties used in the WEPP calibration and simulation

Depth (cm)	Sand (%)	Clay (%)	Organic matter (%)	Bulk density (Mg m ⁻³)	Ks ^a (mm h ⁻¹)	Field capacity (m ³ m ⁻³)	Wilting point (m ³ m ⁻³)	CEC ^b (cmol _c kg ⁻¹)
0–20	8.0	34.8	0.75	1.41	3.7	0.305	0.094	7.5
20–40	7.5	34.8	0.53	1.41	4.6	0.305	0.094	6.0
40–60	7.3	34.8	0.53	1.38	6.3	0.313	0.115	6.0
60–80	7.2	32.9	0.41	1.31	6.7	0.311	0.110	5.8
80–100	8.0	33.3	0.41	1.26	6.8	0.309	0.106	5.8
100–180	9.5	36.8	0.54	1.40	6.8	0.309	0.106	5.8

^a Saturated hydraulic conductivity.

^b Cation exchange capacity.

brated average annual soil loss were 7.2 and 7.6 Mg ha⁻¹, respectively, for continuous soybean, and 9.4 and 9.2 Mg ha⁻¹ for continuous fallow.

Plant growth parameters for maize were taken directly from the WEPP technical documentation (Flanagan and Nearing, 1995) with a biomass-energy conversion ratio of 28 kg MJ⁻¹ to represent the medium fertility level. For winter wheat, the calibrated parameter values were 0.5 for harvest index, 1600 °C day for growing degree day to maturity, 35 kg MJ⁻¹ (high fertility) for biomass-energy conversion ratio, and 1.8 m for rooting depth. The rest of parameter values was taken from Flanagan and Nearing (1995). With the calibrated parameter values, simulated average annual grain yields under the present climate on the 8.7% slope were 3.15 Mg ha⁻¹ for wheat and 6.84 Mg ha⁻¹ for maize, which compared favorably to the regional average yields of 3.16 Mg ha⁻¹ for wheat and 6.44 Mg ha⁻¹ for maize between 1986 and 1999.

2.3. Climate generator (CLIGEN)

The CLIGEN is a stochastic daily weather generator. It generates the occurrence of daily precipitation (related to precipitation frequency) using a first-order, two-state Markov chain based on the transitional probability of a wet day following a wet day (Pw/w) and a wet day following a dry day (Pw/d). The daily precipitation amount is generated using a transformed (skewed) normal distribution (Nicks and Gander, 1994). The daily maximum, minimum, dew point temperatures, and solar radiation are generated using normal distributions. Wind velocity is generated for each of 16 cardinal directions with a transformed normal distribution in each direction. In CLIGEN, daily weather data are generated independently for

each month using the aforementioned distribution for each variable, and each variable is generated independent of other variables. A detailed account of the CLIGEN can be found at <http://horizon.nserl.purdue.edu/Cligen/>.

Since the CLIGEN operates on a monthly basis, each input parameter has 12 values (for 12 months). For each month, input parameters include mean, standard deviation (S), and skew coefficient (SK) of daily precipitation amounts of wet days, and Pw/w, Pw/d, and average maximum 30-min rainfall intensity; means and standard deviations for daily solar radiation and maximum and minimum temperatures; mean for dew point temperature; mean, S, and SK of daily average wind velocity for each of the 16 cardinal directions, which are divided by percent of time in which wind blows from each direction. In addition, an all-time max of 6-h rainfall depth is required by CLIGEN. Values of solar radiation were taken from a neighboring station (200 km northwest of Changwu station), and the rest of parameters were derived from the daily station records of Changwu between 1957 and 2001. These baseline parameter values were input into CLIGEN (v5.111) to generate 100 years of baseline daily weather data to represent present climate, which serves as the basis of comparison for changed climate scenarios. Most baseline parameter values were further modified to generate changed climate.

2.4. Emissions scenario

Climate change experiments conducted by the UK Meteorological Office's Hadley Centre using the HadCM3 model used the emissions scenarios reported in the Special Report on Emissions Scenarios (SRES,

2000) by Intergovernmental Panel on Climate Change (IPCC, <http://www.cru.uea.ac.uk/link/emissions/sres.html>). A set of four families of emissions scenarios was formulated based on future production of greenhouse gases and aerosol precursor emissions. Each scenario described one possible demographic, politico-economic, societal, and technological future. The SRES scenarios of A2a, B2a, and GGA1 were used in this study. Scenario B2a emphasized more environmentally conscious, more regionalized solutions to economic, social, and environmental sustainability. Compared with B2a, scenario A2a also emphasized regionalized solutions to economic and social development, but it was less environmentally conscious. Scenario GGA1 used the historical increase in the individual greenhouse gases from 1860 to 1990 in forcing, and then used the individual increases in greenhouse gases till 2099 as described in the IS92a emissions scenario, which assumed a 1% per year compound rise in radiative forcing. Based on the above emissions scenarios, CO₂ concentration by the year 2085 would increase to 867 ppmv (parts per million by volume) for A2a, 546 ppmv for B2a, and 640 ppmv for GGA1. The IS92a scenario, which was used in the GGA1 forcing, was widely used and considered benchmark in past impact studies.

2.5. *Generating climate change scenario*

Grid cell of HadCM3 experiments is $2.5^{\circ} \times 3.75^{\circ}$ (latitude \times longitude). The four grid cells (between 32.5°N and 37.5°N and from 105°E to 112.5°E) were used in this study (Fig. 1). Note that the study location is on the border of cells A and C near the intersection of the four cells. Due to the independence assumption and the direct use of statistical moments as distribution parameters in CLIGEN, incorporation of GCMs-projected monthly changes in statistical moments into model parameters of daily values becomes straightforward.

Monthly precipitation, mean maximum and minimum temperatures of these four cells between 1950 and 2099 were extracted from the HadCM3 output. The projected hindcasts between 1950 and 1999 were used as control, and data from 2070 to 2099 were referred to as changed climates. The selection of the 2070–2099 period was to simulate the potential impact of climate change on natural resources by

the end of the century. The 30-year period was considered long enough to allow reliable estimation of climate parameters while minimizing the undesirable effects of climate nonstationarity on those estimates. Overall means and variances of monthly precipitation and temperatures were calculated for each period and cell. Mean temperature shifts, temperature variance ratios, precipitation ratios, and precipitation variance ratios between the two periods were calculated for each month and cell. To capture the potential variability of regional responses of surface hydrology and soil erosion to climate change, arithmetic means of the relative changes were also calculated for cells A and C as well as for all four cells.

The precipitation-related baseline parameters including Pw/w, Pw/d, mean and variance of daily precipitation of wet days were adjusted as follows. For each month, future transitional probabilities of precipitation were estimated for projected monthly means from linear relationships developed using historical transitional probability and monthly precipitation at the Changwu station. The projected monthly means were obtained by multiplying mean ratios of GCM-projected monthly precipitation between 2070–2099 and 1950–1999 by the baseline monthly precipitation means measured during 1956–2001 at the Changwu station. The mean daily precipitation per wet day, which is a CLIGEN input parameter, was analytically computed using the adjusted transitional probabilities, projected monthly mean, and number of days in the month. New variances of daily precipitation under climate change, which is another input parameter for CLIGEN, was approximated by multiplying the baseline variances derived from the daily station records by the monthly variance ratios between the target and control periods under the assumptions that transitional probabilities and autocorrelation of daily precipitation in both baseline and changed climates are similar.

Projected mean maximum and minimum temperature shifts were directly added to the corresponding baseline means as was used by other modelers (e.g., Wilks, 1992; Mearns et al., 1997; Katz, 1996). Adjusted daily temperature variances were obtained by multiplying the baseline temperature variances by the calculated variance ratios. This method is appropriate if autocorrelation coefficients of all orders in the baseline are similar to those in the changed

climates (Katz, 1985). Readers are referred to the article of Zhang et al. (2004) for detailed derivation and test of the downscaling method. All new parameter values were then input into CLIGEN, and 100 years of daily weather data were generated for each of three emission scenarios and at three spatial scales.

2.6. Simulated agronomic systems

All measured soil properties including saturated hydraulic conductivity (3.7 mm h^{-1} in the top 20-cm layer) and the configurations of the two runoff plots, which were used in the WEPP model calibration, were used in the climatic impact simulation. Overall mean of measured storm duration at Changwu station was 2.88 times that of CLIGEN-generated storm durations (note that storm duration is not a CLIGEN input parameter and therefore is not calibrated to the Changwu location). To adjust this bias, a factor of 2.88 was multiplied to CLIGEN-generated storm durations and relative peak intensities (defined as a ratio of instant peak rainfall intensity to average storm intensity) in both baseline and changed climates. A common regional three-year rotation of wheat–wheat–maize was selected. In the simulation under the baseline climate condition, winter wheat was planted on September 23 and harvested on June 27 of the following year; and maize was planted on April 15 and harvested on September 22. However, under the changed climates, wheat was planted 10 days later and harvested 10 days earlier; and maize was planted 10 days earlier and harvested 15 days earlier to

accommodate the increased temperature. Two tillage and residue management systems were simulated. For the common traditional system, 90% of crop residue was removed and field was moldboard plowed one week after harvest. For a conservation system with delayed tillage operation, residue was left in place after harvest and the field was moldboard plowed one week before planting. The two 20-m long plots at an 8.7% and 17.6% slope, which were used in the model calibration, were used in the simulation.

3. Results and discussion

3.1. Projected climate change

3.1.1. Precipitation

Projected mean annual precipitation during 2070–2099 compared with 1950–1999 would increase by 120, 157, 186, and 214 mm (equivalent to 27, 31, 16, and 28% increase) for cells A, B, C, and D (Fig. 1), respectively, for the A2a scenario; increase by 148, 159, 158, and 159 mm (33, 32, 14, and 21%) for B2a; and increase by 150, 168, 208, and 160 mm (30, 29, 17, and 19%) for GGa1. The projected percent increases in precipitation varied with emission scenarios and in space. To better account for the spatial variability and to assess the first order regional responses of surface hydrology and soil erosion to climate change, the percent changes at three spatial scales were calculated (Table 2) and used to modify baseline precipitation parameters to generate three climate changes for each emission scenario. Note that

Table 2
Averaged annual climate perturbations at three spatial scales between 1950–1999 and 2070–2099

Emissions scenario	Grid cells averaged	Precipitation		Maximum temperature		Minimum temperature	
		Change (%)	M.V.R. ^a	Shift (°C)	M.V.R.	Shift (°C)	M.V.R.
A2a	A	26.7	1.627	3.96	1.145	5.25	1.133
	AC	21.5	1.634	4.25	1.315	4.98	1.192
	ABCD	25.5	1.724	4.03	1.141	4.88	1.258
B2a	A	33.3	1.606	2.33	1.101	3.89	0.989
	AC	23.7	1.406	2.80	1.143	3.66	0.959
	ABCD	25.1	1.397	2.58	1.042	3.61	0.967
GGa1	A	29.9	1.886	3.34	0.944	4.53	1.020
	AC	23.6	1.684	3.62	0.962	4.26	0.952
	ABCD	24.0	1.725	3.55	0.903	4.23	0.938

^a M.V.R. = average monthly variance ratio of 2070–2099 over 1950–1999.

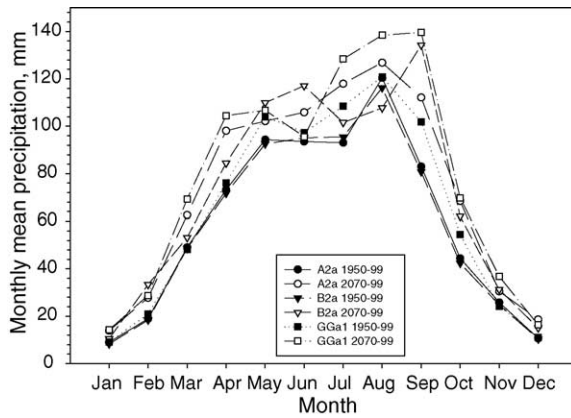


Fig. 2. HadCM3-projected monthly mean precipitation for the periods of 1950–1999 (hindcast) and 2070–2099 for three emissions scenarios. Data are the means of the four grid cells.

the projected precipitation variances, which varied slightly in space, would be 1.4–1.9 times greater in 2070–2099 than in 1950–1999. The greater variance would result in greater numbers of larger storms, and therefore greater soil loss.

Projected monthly mean precipitation amounts (Fig. 2), and mean and variance ratios of projected monthly precipitation between 2070–2099 and 1950–1999 (Fig. 3) as averaged over the four grid cells are presented as an example to show the seasonal trends of projected climate change for the three emission scenarios. In general, three emission scenarios projected more precipitation increases in the spring and summer than in the winter and fall (Fig. 2). However, the opposite was true for the relative increases in precipitation (Fig. 3A). Parallel to the seasonal trends of mean precipitation ratios, variance ratios exhibited greater increases in winter months (Fig. 3B). Larger increases in precipitation variance in winter months would not result in considerable increases in soil loss due to small amounts of monthly total precipitation (Fig. 2). Conversely, smaller increases in variance in July–September, in which more than 95% soil erosion occurred, would cause considerable soil loss. The A2a scenario projected the most increases in these three months, while B2a projected the least increases (note a dramatic decrease in August) with moderate increases for GGA1. These variance changes would have substantial effect on simulated soil loss as is shown later.

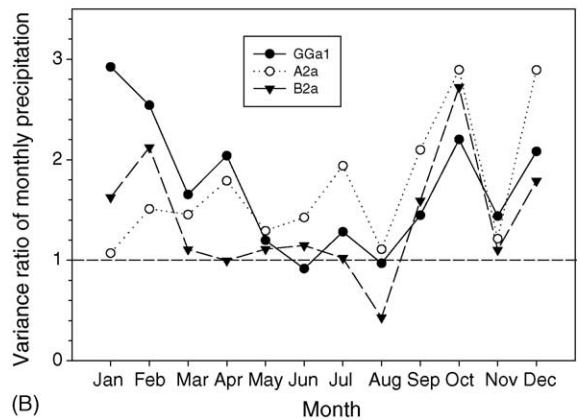
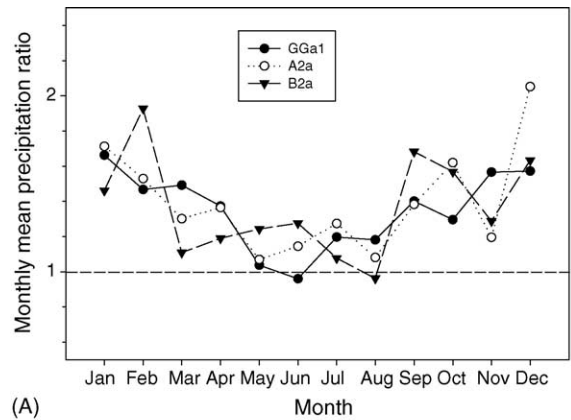


Fig. 3. (A) Ratios of HadCM3-projected monthly mean precipitation and (B) variance ratios of projected monthly precipitation between 1950–1999 and 2070–2099 under three emissions scenarios. Data are the means of the four grid cells. Note that 1 means no change and greater than 1 means an increase.

3.1.2. Temperature

The spatial variation for temperature was much less than that for precipitation. Projected mean annual temperature during 2070–2099 compared with 1950–1999 would increase by 4.65, 4.25, 4.60, and 4.30 °C for cells A, B, C, and D, respectively, for the A2a scenario; increase by 3.10, 2.85, 3.35, and 3.05 °C for B2a; and increase by 3.90, 3.75, 3.95, and 3.95 °C for GGA1. The A2a scenario projected the most temperature increase, while B2a projected the least increase, with moderate increase for GGA1. Minimum temperature increased more than maximum temperature in all the three emission scenarios (Table 2). Projected overall variance of monthly temperature was slightly

increased for A2a, somewhat unchanged for B2a, and slightly decreased for GGa1 (Table 2).

Seasonal patterns of temperature increase and variance change are shown in Figs. 4 and 5. There were two peaks of temperature increase: one in the summer and the other in the winter. Generally, projected mean temperature rises were greatest throughout the year in A2a, and lowest in B2a, with GGa1 being in between. For temperature variance, A2a projected increases (variance ratio >1) for most months for both minimum and maximum temperatures, while B2a and GGa1 projected both increases and decreases without consistent patterns throughout the year. Mearns (1996) reported that variance change in temperature could have a substantial effect on

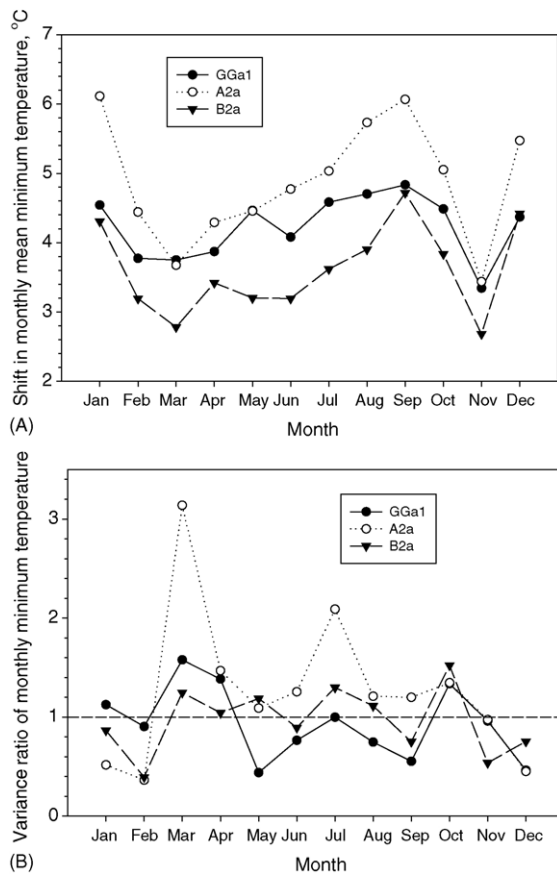


Fig. 4. Shifts (A) and variance ratios (B) of HadCM3-projected monthly mean minimum temperature between 1950–1999 and 2070–2099 under three emissions scenarios. Data are the means of the four grid cells.

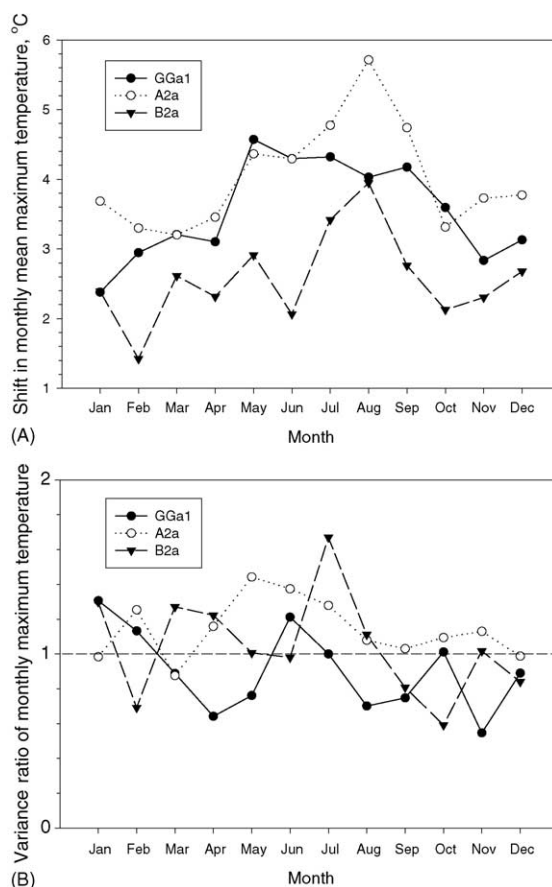


Fig. 5. Shifts (A) and variance ratios (B) of HadCM3-projected monthly mean maximum temperature between 1950–1999 and 2070–2099 under three emissions scenarios. Data are the means of the four grid cells.

simulated wheat yields in Kansas. However, Zhang et al. (2004) found that GCM-projected variance change in temperature had little effect on simulated runoff, soil loss, and wheat production at El Reno, Oklahoma.

3.2. Response to climate change in conventional tillage systems

3.2.1. Surface runoff and soil loss

Predicted mean annual precipitation, runoff, soil loss, grain yield, and their percent changes relative to the baseline climate scenario are presented in Table 3. Please note that the percent precipitation changes in Table 2 are different from those in Table 3, which were

Table 3

Predicted mean annual precipitation, runoff, soil loss, grain yield as well as their percent changes relative to the corresponding slope in the baseline scenario for Changwu, China at three spatial scales under conventional tillage in a wheat–wheat–maize rotation^a

Slope (%)	Grid cell averaged	Precipitation		Runoff		Soil loss		Wheat grain		Maize grain	
		Depth (mm)	Change (%)	Depth (mm)	Change (%)	Rate (Mg ha ⁻¹)	Change (%)	Yield (Mg ha ⁻¹)	Change (%)	Yield (Mg ha ⁻¹)	Change (%)
Baseline scenario of Changwu Station at 350 ppmv CO ₂											
8.7		579	0	45	0	3.1	0	3.3	0	7.0	0
17.6		579	0	55	0	9.4	0	3.1	0	6.8	0
Scenario A2a at 867 ppmv CO ₂											
8.7	A	766	32	74	63	4.9	57	4.1	26	11.3	61
8.7	AC	722	25	81	78	5.6	79	3.6	11	10.5	50
8.7	ABCD	749	29	89	96	6.5	107	3.5	7	11.1	59
17.6	A	766	32	86	56	15.0	60	3.8	21	11.2	64
17.6	AC	722	25	93	69	16.4	74	3.5	11	10.3	50
17.6	ABCD	749	29	101	83	18.4	95	3.4	8	10.9	60
Scenario B2a at 546 ppmv CO ₂											
8.7	A	796	37	68	49	3.6	14	5.1	58	11.3	61
8.7	AC	734	27	54	20	2.9	-7	4.4	36	10.4	49
8.7	ABCD	738	27	57	25	3.1	0	4.4	36	10.5	51
17.6	A	796	37	80	44	11.0	17	4.9	58	11.2	64
17.6	AC	734	27	65	19	9.4	0	4.3	36	10.3	50
17.6	ABCD	738	27	68	23	10.1	7	4.3	37	10.4	53
Scenario GGa1 at 640 ppmv CO ₂											
8.7	A	752	30	65	42	4.5	43	4.5	39	10.3	47
8.7	AC	716	24	63	38	4.3	36	4.1	25	9.8	40
8.7	ABCD	712	23	69	52	4.7	50	3.9	21	9.2	32
17.6	A	752	30	76	37	12.8	36	4.4	39	10.2	49
17.6	AC	716	24	75	35	12.8	36	3.9	24	9.7	41
17.6	ABCD	712	23	80	46	14.1	50	3.8	21	9.1	33

^a 90% residue was removed and soil was moldboard plowed within one week after each harvest in a wheat–wheat–maize rotation.

averaged by weighting the GCM-projected relative monthly changes by the corresponding baseline mean monthly precipitation at Changwu. The percentages in Table 2 were directly calculated using the raw GCM-annual precipitation in the cells. Also, to side step the derivation of the skillful resolution for the region, the impact assessment was conducted and reported at three spatial scales (one, two, and four grid cells). Such an approach would yield an ensemble of possible responses to climate change in the region, which indicates potential variability including not only the more regionalized first-order responses at multiple grids but also the localized responses at single grid (Zhang, 2005).

The three emissions scenarios projected similar precipitation increases during 2070–2099 at Changwu, ranging from 23% to 37% over the three spatial scales (Table 3). Projected runoff increases in

the conventional tillage systems under changed climates, compared with the present climate, varied from 19% under B2a at grid AC at the 17.6% slope to 96% under A2a at grid ABCD at the 8.7% slope. The overall averaged runoff increases were greatest under A2a, least under B2a, and intermediate under GGa1. Predicted runoff depths were consistently greater at the 17.6% slope than at the 8.7% slope, indicating smaller surface retention storage at higher slopes. Predicted relative soil loss increases were much more variable than predicted relative runoff increases, ranging from -7% under B2a at grid AC at the 8.7% slope to 107% under A2a at grid ABCD at the 8.7% slope. At the same slope and spatial scale, predicted soil loss increases were greatest under A2a, least under B2a, and intermediate under GGa1. The least soil loss increase in B2a was because of (i) the least increase in surface runoff and the most increase

in wheat yield and (ii) the least increase in precipitation variance in July and August (Fig. 3B), during which most soil erosion occurred (35% of measured soil loss occurred in July and 65% in August from 1988 to 1992). As mentioned earlier, larger precipitation variance leads to more frequent occurrence of heavy storms, which in turn result in more severe soil erosion. The percent soil loss increases averaged over the three spatial scales were 81%, 2%, and 43% under A2a, B2a, and GGal, respectively, at the 8.7% slope; and were 76%, 8%, and 41% at the 17.6% slope. Although absolute soil loss rates at the 17.6% slope were about three times greater than those at the 8.7% slope, predicted relative soil loss increases were similar. Overall, soil loss increased for all three climate change scenarios despite increased wheat and maize yields. This was mainly because of increased precipitation variability, increased runoff, and short-

tened growing season due to temperature rises under climate changes.

3.2.2. Grain yield

Predicted wheat grain yield under changed climates, compared with the present climate, increased from 7% under A2a at grid ABCD at the 8.7% slope to 58% under B2a at grid A at the 8.7% slope. The relative increases averaged across the three spatial scales and two slopes were 14%, 43%, and 28% under A2a, B2a, and GGal, respectively. The overall increase under all three scenarios was attributed to the considerable increase in precipitation, which is the major limiting factor for agricultural production in the region. The more increase in the B2a scenario was partially because lower temperature rise was projected for the scenario (Table 2). Predicted maize grain yields increased from 32% under GGal at grid ABCD at the

Table 4

Predicted mean annual plant transpiration, soil evaporation, percolation to below 1.8 m, averaged daily soil moisture in 1.8-m soil profile as well as their percent changes relative to the corresponding slope in the baseline scenario for Changwu, China at three spatial scales under conventional tillage in a wheat–wheat–maize rotation^a

Slope (%)	Grid cell averaged	Transpiration		Evaporation		Percolation	Soil moisture	
		Depth (mm)	Change (%)	Depth (mm)	Change (%)		Depth (mm)	Depth (mm)
Baseline scenario of Changwu Station at 350 ppmv CO ₂								
8.7		355	0	182	0	0.6	300	0
17.6		349	0	178	0	0.6	296	0
Scenario A2a at 867 ppmv CO ₂								
8.7	A	461	30	232	28	2.6	320	7
8.7	AC	431	22	212	17	0.6	304	1
8.7	ABCD	442	25	218	20	2.2	312	4
17.6	A	455	30	227	28	1.9	315	7
17.6	AC	424	21	207	17	0.6	299	1
17.6	ABCD	435	25	213	20	1.8	307	4
Scenario B2a at 546 ppmv CO ₂								
8.7	A	473	33	251	38	6.2	346	16
8.7	AC	441	24	238	31	2.2	332	11
8.7	ABCD	442	25	239	31	2.4	334	11
17.6	A	466	34	247	39	5.1	341	15
17.6	AC	434	24	234	32	1.8	327	11
17.6	ABCD	435	25	235	32	1.9	329	11
Scenario GGal at 640 ppmv CO ₂								
8.7	A	461	30	227	25	1.7	317	6
8.7	AC	435	23	219	21	1.4	312	4
8.7	ABCD	431	21	214	18	1.2	308	3
17.6	A	455	30	223	25	1.3	312	6
17.6	AC	428	23	214	21	1.2	307	4
17.6	ABCD	424	22	209	18	1.0	304	3

^a 90% residue was removed and soil was moldboard plowed within one week after each harvest in a wheat–wheat–maize rotation. On average, less than 0.04-mm water was laterally transported downslope each year.

8.7% slope to 64% under A2a at grid A at the 17.6% slope. The overall averaged increases were 57% for A2a, 54% for B2a, and 40% for GGa1. In general, predicted relative yield increases were consistently greater for maize than for wheat under all three scenarios. The greater increase for maize was because (i) projected precipitation increases were greater in the maize growing season than in the wheat growing season (Fig. 2), (ii) temperature rise diminished wheat yields more than maize yields, and (iii) maize was more responsive to CO₂ increase than winter wheat. Supplemental model runs were made under the conditions identical to the baseline climate except that the monthly mean temperatures were elevated by 2.2 °C or 4.4 °C for each month. The results showed that for a 2.2 °C increase wheat grain yield decreased by 14% but maize yield increased by 1%, and for a 4.4 °C increase wheat and maize grain yield decreased by 31% and 17%, respectively. The WEPP model was also run under the baseline climate but for the doubled CO₂ concentration, the results showed that for each 10% increase in CO₂ wheat yield increased by 1% while maize yield increased by 4%. The greater increase with CO₂ for maize was an integrated effect

of crop characteristics and environmental conditions at the station.

3.2.3. ET and soil water balance

Predicted mean annual plant transpiration, soil evaporation, percolation, and long-term soil moisture balance in the 1.8-m soil profile under the conventional tillage are shown in Table 4. Compared with the baseline conditions, plant transpiration increased from 21 to 34% across all emissions scenarios, spatial scales, and slopes. The percent increases averaged across all spatial scales and slopes were 25% for A2a, 28% for B2a, and 25% for GGa1. The greatest increase for B2a was largely due to the greatest increase in predicted precipitation and the best performance of winter wheat (Table 3). The slope steepness had negligible effect on transpiration, soil evaporation, and soil moisture balance. Within each emissions scenario, the greatest transpiration was predicted at grid A, which was consistent with the largest increases in grain yield and precipitation at grid A.

The overall averaged percent increases of soil evaporation were 22% for A2a, 34% for B2a, and 21%

Table 5

Predicted mean annual runoff, soil loss, grain yield as well as their percent changes in conservation tillage under changed climates relative to the conventional tillage in the baseline scenario for Changwu, China at the 17.6% slope in a wheat–wheat–maize rotation at three spatial scales^a

Grid cell averaged	Runoff		Soil loss		Wheat grain		Maize grain	
	Depth (mm)	Change (%)	Rate (Mg ha ⁻¹)	Change (%)	Yield (Mg ha ⁻¹)	Change (%)	Yield (Mg ha ⁻¹)	Rate (Mg ha ⁻¹)
Baseline scenario at 350 ppmv CO ₂ , conventional tillage	55	0	9.4	0	3.1	0	6.8	0
Scenario A2a at 867 ppmv CO ₂ , conservation tillage								
A	39	-29	3.6	-62	4.2	33	10.9	59
AC	45	-18	4.0	-57	3.8	19	10.1	48
ABCD	52	-7	4.9	-48	3.6	16	10.9	59
Scenario B2a at 546 ppmv CO ₂ , conservation tillage								
A	40	-28	3.1	-67	5.1	61	10.9	59
AC	31	-44	2.9	-69	4.3	38	9.6	41
ABCD	32	-42	3.4	-64	4.3	36	9.8	44
Scenario GGa1 at 640 ppmv CO ₂ , conservation tillage								
A	36	-35	3.4	-64	4.4	40	9.6	40
AC	35	-36	3.4	-64	4.0	26	9.1	33
ABCD	39	-30	3.8	-60	3.9	23	8.7	27

^a 90% residue was removed and soil was moldboard plowed within one week after each harvest in the conventional tillage; residue was left in place after harvest and soil was moldboard plowed one week before planting in the conservation tillage.

for GGA1. The greatest increase for B2a was largely because of the wettest soil profiles (Table 4), which resulted from more precipitation increase in the scenario. Within each emissions scenario, the greatest soil evaporation occurred at grid scale A, because the greatest increases in soil moisture reserve and precipitation were predicted at the scale. The trends of the relative soil moisture changes between the emissions scenarios as well as between the spatial scales within each scenario were similar to those of soil evaporation, simply because soil evaporation was mainly limited by soil water supply rather than by evaporative demand in the study region. The long-term daily soil moisture balance in the 1.8-m soil profile would increase by 4% for A2a, 12% for B2a, and 4% for GGA1. The surplus in the soil water balance indicates that an additional summer crop such as broom-corn millet can be grown following the second year wheat in the common wheat–wheat–maize rotation to take advantage of additional plant available water under climate change. The broom-corn millet, which is presently grown in years when soil

moisture is sufficient, would increase the efficient use of rainwater by reducing runoff, deep percolation, and soil evaporation. Compared with the baseline condition, deep percolation loss (or subsoil/groundwater recharge) was generally increased under the changed climate, mostly ranging from 1 to 6 mm. The maximum recharge occurred at grid A under B2a, where the most rainfall increase was predicted. The lateral movement of soil water downslope under the changed climate was less than 0.04 mm per year on average, and therefore this component was excluded from Table 4.

3.3. Response to climate change under conservation tillage

3.3.1. Surface runoff, soil loss, and grain yield

Predicted mean annual changes in hydrology, soil erosion, and grain yield under the conservation tillage at the 17.6% slope are presented in Tables 5 and 6. The only difference between the conservation and conventional tillage is that the timing of crop residue

Table 6

Predicted mean annual plant transpiration, soil evaporation, percolation to below 1.8 m, and averaged daily soil moisture in 1.8-m soil profile in the conservation tillage under changed climates, as well as their percent changes relative to those under the conventional tillage in the baseline scenario for Changwu, China at the 17.6% slope at three spatial scales^a

Grid cell averaged	Transpiration		Evaporation		Percolation Depth (mm)	Soil moisture	
	Depth (mm)	Change (%)	Depth (mm)	Change (%)		Depth (mm)	Change (%)
Changwu baseline at 350 ppmv CO ₂ , conventional tillage	349	0	178	0	0.6	296	0
Scenario A2a at 867 ppmv CO ₂ , conservation tillage							
A	458	31	269	51	3.8	316	7
AC	432	24	246	39	1.1	303	3
ABCD	443	27	253	43	3.0	313	6
Scenario B2a at 546 ppmv CO ₂ , conservation tillage							
A	469	34	285	60	4.5	337	14
AC	430	23	274	54	1.7	319	8
ABCD	431	24	275	55	1.7	320	8
Scenario GGA1 at 640 ppmv CO ₂ , conservation tillage							
A	452	29	266	50	0.9	306	4
AC	425	22	257	44	1.2	303	3
ABCD	422	21	252	42	1.1	300	2

^a 90% residue was removed and soil was moldboard plowed within one week after each harvest in the conventional tillage; residue was left in place after harvest and soil was moldboard plowed one week before planting in the conservation tillage. On average, less than 0.3-mm water was laterally transported downslope each year.

Table 7

Percent increases of selected variables for each percent increase in precipitation (sensitivity) under the conventional tillage, as calculated between the changed and present climates and averaged over three spatial scales for each slope and emissions scenario

Slope (%)	Emissions scenario	Runoff	Soil loss	Wheat yield	Maize yield	Plant transpiration	Soil evaporation
8.7	A2a	2.76	2.82	0.54	1.98	0.89	0.75
8.7	B2a	1.04	0.08	1.46	1.75	0.90	1.10
8.7	GGa1	1.74	1.69	1.11	1.56	0.97	0.83
17.6	A2a	2.42	2.66	0.52	2.01	0.89	0.75
17.6	B2a	0.94	0.26	1.42	1.83	0.90	1.10
17.6	GGa1	1.56	1.59	1.09	1.60	0.98	0.83

removal and tillage operation. The 90% of crop residue was removed and fields were moldboard plowed within one week of harvest under the conventional tillage, but they were delayed to within one week before planting of the next crop under the conservation. In contrast with the relative increase under the conventional tillage, surface runoff was reduced by 7–44% under the conservation tillage under all emissions scenarios (Table 5). The average runoff reduction was 18% for A2a, 38% for B2a, and 34% for GGa1. It is well documented that surface residue cover is effective in reducing surface runoff and erosion by dissipating raindrop energy, controlling soil crust formation, and obstructing overland flow (Mannering and Meyer, 1963). As a result of runoff reduction and residue protection, soil losses were dramatically reduced under the conservation tillage under all scenarios, reversing the increasing trend under the conventional tillage. The average soil loss reduction, compared with the conventional tillage under the baseline climate, was 56% for A2a, 67% for B2a, and 63% for GGa1. Predicted wheat and maize yields were more or less similar to those under the conventional tillage, with wheat being slightly higher and maize slightly lower.

3.3.2. ET and soil water balance

Predicted mean annual plant transpiration under the conservation tillage was similar to those under the conventional tillage under all emissions scenarios at the 17.6% slope (Table 6). The percent increases averaged over all three spatial scales were 27% for A2a, 27% for B2a, and 24% for GGa1. Soil evaporation under the conservation tillage was about two times that under the conventional tillage. Soil evaporation under the conservation tillage included evaporation of soil water and residue-intercepted rainwater. Greater evaporation with residue cover may

suggest residue interception was overestimated and/or residue suppression on direct soil evaporation was underestimated in the WEPP model. This finding needs to be further evaluated using measured evaporation data. The deep percolation depths were comparable with those under the conventional tillage, ranging from 1 mm to 5 mm per year. The long-term daily soil moisture balance in the 1.8-m soil profile were also similar to those under the conventional tillage, showing an overall increase of 5% for A2a, 10% for B2a, and 3% for GGa1.

4. Conclusions and implications

The Hadley Centre model (HadCM3) predicted a 23–37% increase in annual precipitation, 2.3–4.3 °C rise in maximum temperature, and 3.6–5.3 °C rise in minimum temperature for the region over the century. Variance of daily precipitation was predicted to increase, especially under the A2a and GGa1 scenarios. As a result of precipitation increase, surface runoff, soil loss, ET, and crop yield would generally increase as predicted by the WEPP model in the conventional tillage systems. Compared with the baseline climate, predicted percent increases under climate changes, as averaged over the three spatial scales for each emissions scenario and slope, ranged from 29 to 79% for runoff, 2 to 81% for soil loss, 15 to 44% for wheat grain yield, 40 to 58% for maize yield, 25 to 28% for crop transpiration, 21 to 34% for soil evaporation, and 4 to 12% for long-term soil water reserve under the conventional tillage in a common wheat–wheat–corn rotation. However, adoption of the conservation (delayed) tillage would reduce runoff by 18–38%, and decrease soil loss by 56–68% compared with the conventional tillage under the baseline climate. Predicted plant transpiration, soil evaporation, crop yield, and soil moisture balance under

climate change were little affected by the tillage systems.

Model simulation under the baseline and changed climates in the conventional tillage systems indicated that each percent increase in future precipitation would, on average, result in 1.0–2.8% increase in surface runoff, 0.1–2.8% increase in soil loss, 0.5–1.5% increase in wheat grain yield, 1.6–2.0% increase in maize yield, 0.9–1.0% increase in plant transpiration, and 0.8–1.1% increase in soil evaporation (Table 7). The sensitivities of surface runoff and soil loss to precipitation change were within the range reported in the literature (e.g., Favis-Mortlock and Savabi, 1996; Savabi et al., 1993; Pruski and Nearing, 2002a,b; Favis-Mortlock et al., 1991; Boardman and Favis-Mortlock, 1993). The significant increases in predicted wheat and maize yields were results of increased precipitation and CO₂ concentration, which outweighed the negative effect of temperature rise on crop growth.

It is for the first time that CLIGEN was used in China. It is fairly easy to develop CLIGEN input parameters from long-term meteorological station data. Preliminary application of CLIGEN to the Changwu station on southern Loess Plateau in this study indicates that CLIGEN is readily applicable to the region. However, the generated mean storm duration was about half the mean storm duration measured at Changwu. Applicability of CLIGEN needs to be further evaluated in more detail using measured climate data at more stations.

Acknowledgements

This work was partially supported by a grant of National Natural Science Foundation of China, No. 90202011. The GCM data were supplied by the Climate Impacts LINK Project (DEFRA Contract EPG I/1/124) on behalf of the Hadley Centre and U.K. Meteorological Office.

References

- Boardman, J., Favis-Mortlock, D.T., 1993. Climate change and soil erosion in Britain. *Geographical J.* 159 (2), 179–183.
- Chen, Y.Z., Jing, K., Cai, J.G., 1988. *Modern Soil Erosion and Conservation on the Loess Plateau* (in Chinese). Science Press, Beijing, PR China, p. 194.
- Edwards, W.M., Owens, L.B., 1991. Large storm effects on total soil erosion. *J. Soil Water Conserv.* 46 (1), 75–78.
- Favis-Mortlock, D.T., Evans, R., Boardman, J., Harris, T.M., 1991. Climate change, winter wheat yield, and soil erosion on the English South Downs. *Agric. Syst.* 37, 415–433.
- Favis-Mortlock, D.T., Savabi, M.R., 1996. Shifts in rates and spatial distribution of soil erosion and deposition under climate change. In: Anderson, M.G., Brooks, S.M. (Eds.), *Advances in Hillslope Processes*. John Wiley, New York, pp. 529–560.
- Flanagan, D.C., Nearing, M.A. (Eds.), 1995. *USDA-Water Erosion Prediction Project: Hillslope Profile and Watershed Model Documentation*. NSERL Report No. 10. West Lafayette, Ind.: USDA-ARS Nat. Soil Erosion Research Lab.
- Gordon, C., Cooper, C., Senior, C.A., Banks, H., Gregory, J.M., Johns, T.C., Mitchell, F.B., Wood, R.A., 2000. The simulation of SST, sea ice extents and ocean heat transports in a version of the Hadley Centre coupled model without flux adjustments. *Clim. Dyn.* 16, 147–168.
- Hansen, J.W., Indeje, M., 2004. Linking dynamic seasonal climate forecasts with crop simulation for maize yield prediction in semi-arid Kenya. *Agric. For. Meteorol.* 125, 143–157.
- Hewitson, B., 2003. Developing perturbations for climate change impact assessments, *Transactions of American Geophysical Union*. EOS 84 (35), 337–348.
- IPCC (Intergovernmental Panel on Climate Change), Working Group I, 2001. *Climate Change 2001: The scientific basis*. Contribution of Working Group I to the Third Assessment Report of the IPCC. Cambridge University Press, Cambridge, UK.
- Katz, R.W., 1985. Probabilistic models. In: Murphy, A.H., Katz, R.W. (Eds.), *Probability, Statistics, and Decision Making in the Atmospheric Sciences*. Westview, pp. 261–288.
- Katz, R.W., 1996. Use of conditional stochastic models to generate climate change scenarios. *Clim. Change* 32, 237–255.
- Mannering, J.V., Meyer, L.D., 1963. The effects of various rates of surface mulch on infiltration and erosion. *Soil Sci. Soc. Am. Proc.* 27 (1), 84–86.
- Mavromatis, T., Hansen, J.W., 2001a. Interannual variability characteristics and simulated crop response of four stochastic weather generators. *Agric. For. Meteorol.* 109, 283–296.
- Mavromatis, T., Hansen, J.W., 2001b. Interannual variability characteristics and simulated crop response of four stochastic weather generators. *Agric. For. Meteorol.* 109, 283–296.
- Mavromatis, T., Jones, P.D., 1998. Comparison of climate change scenario construction methodologies for impact assessment studies. *Agric. For. Meteorol.* 91, 51–67.
- Mearns, L.O., Rosenzweig, C., Goldberg, R., 1997. Mean and variance change in climate scenarios: Methods, agricultural applications, and measures of uncertainty. *Clim. Change* 35, 367–396.
- Mearns, L.O., 1996. The effect of changes in daily and interannual climatic variability on CERES-Wheat: a sensitivity study. *Clim. Change* 32, 257–292.
- Nicks, A.D., Gander, G.A., 1994. CLIGEN: a weather generator for climate inputs to water resource and other models. In: *Proceed-*

- ings of the 5th International Conference on Computers in Agriculture, American Society of Agricultural Engineers, St. Joseph, Michigan, pp. 3–94.
- Pope, V.D., Gallani, M.L., Rowntree, P.R., Stratton, R.A., 2000. The impact of new physical parameterizations in the Hadley Centre Climate Model—HadAM3. *Clim. Dyn.* 16, 123–146.
- Pruski, F.F., Nearing, M.A., 2002a. Runoff and soil-loss responses to changes in precipitation: a computer simulation study. *J. Soil Water Conserv.* 57 (1), 7–16.
- Pruski, F.F., Nearing, M.A., 2002b. Climate-induced changes in erosion during the 21st century for eight U.S. locations. *Water Resour. Res.* 38 (12) art. no. 1298.
- Rosenzweig, C., Parry, M.L., 1994. Potential impact of climate change on world food supply. *Nature* 367, 133–137.
- Savabi, M.R., Arnold, J.G., Nicks, A.D., 1993. Impact of global climate change on hydrology and soil erosion: a modeling approach. In: Eckstein, Y., Zaporozec, A. (Eds.), *Proceedings of Industrial and Agricultural Impact of Environmental and Climatic Change on Global and Regional Hydrology*, Water Environment Federation, Alexandria, Virginia, pp. 3–18.
- Semenov, M.A., Porter, J.R., 1995. Climatic variability and the modeling of crop yields. *Agric. For. Meteorol.* 73, 265–283.
- Solman, S., Nuñez, M., 1999. Local estimates of global climate change: a statistical downscaling approach. *Int. J. Climatol.* 19, 835–861.
- SWCS, 2003. Conservation implications of climate change: soil erosion and runoff from cropland. A report from the Soil and Water Conservation Society. Soil and Water Conservation Society, Ankeny, Iowa (www.swcs.org/docs/climate#change-final.pdf).
- Wilby, R.L., Wigley, T.M.L., Conway, D., Jones, P.D., Hewitson, B.C., Main, J., Wilks, D.S., 1998. Statistical downscaling of general circulation model output: a comparison of methods. *Water Resour. Res.* 34, 2995–3008.
- Wilks, D.S., 1992. Adapting stochastic weather generation algorithms for climate change studies. *Clim. Change* 22, 67–84.
- Wood, R.A., Keen, A.B., Mitchell, J.F.B., Gregory, J.M., 1999. Changing spatial structure of the thermohaline circulation in response to atmospheric CO₂ forcing in a climate model. *Nature* 399, 572–575.
- Zhang, G.H., Nearing, M.A., Liu, B.Y., 2005. Potential effects of climate change on rainfall erosivity in the Yellow River basin of China. *Trans. ASAE* 48, 511–517.
- Zhang, X.C., Garbrecht, J.D., 2002. Precipitation retention and soil erosion under varying climate, land use, tillage, and cropping systems. *J. Am. Water Resour. Assoc.* 38, 1241–1253.
- Zhang, X.C., Nearing, M.A., Garbrecht, J.D., Steiner, J.L., 2004. Downscaling monthly forecasts to simulate impacts of climate change on soil erosion and wheat production. *Soil Sci. Soc. Am. J.* 68, 1376–1385.
- Zhang, X.C., 2005. Spatial sensitivity of predicted soil erosion and runoff to climate change at regional scales. *J. Soil Water Conserv.* (in review).